JETP Letters, Vol. 78, No. 7, 2003, pp. 443–446. Translated from Pis'ma v Zhurnal Éksperimental'noĭ i Teoreticheskoĭ Fiziki, Vol. 78, No. 7, 2003, pp. 911–914.

Statistics of Eigenfunctions of Chaotic Billiards Taking Account of the Rashba Spin–Orbit Interaction

E. N. Bulgakov and A. F. Sadreev

Kirenskiĭ Institute of Physics, Siberian Division, Russian Academy of Sciences, Akademgorodok, Krasnoyarsk, 660036 Russia

Received July 21, 2003; in final form, August 28, 2003

It is demonstrated, both analytically and numerically, that eigenfunction statistics in chaotic billiards with spin–orbit interaction fundamentally depend on the ratio of the squared spin–orbit interaction constant. If this ratio is small, one of the eigenstate components is a random Gaussian field, whereas another is not universal and depends on the billiard type. In the opposite case, the statistics of both components is described by the independent random complex Gaussian fields with the same variances. In the intermediate case, both eigenfunction components do not satisfy Gaussian statistics. © *2003 MAIK "Nauka/Interperiodica".*

PACS numbers: 05.45.Mt; 73.21.La

In typical III–V semiconductor heterostructures, electrons form two-dimensional electron gas between layers [1, 2]. At helium temperatures, the coherence length is as high as several microns. By appropriately choosing the shape of surface electrode, one can confine electrons in an arbitrarily shaped quantum dot, which will be called a two-dimensional billiard. Such heterostructures are characterized by the Rashba spin–orbit interaction (SOI) [3], which modifies the Hamiltonian as

$$H = \frac{-\hbar^2}{2m^*}\nabla^2 + \hbar K[\sigma \times \mathbf{p})]_z, \qquad (1)$$

where m^* is the electron effective mass. The SOI constant K is proportional to the averaged interface electric field $\langle E\rangle = \langle -(1/e)(dE_c/dz) + E_i\rangle$, where E_c is the conduction band profile along the z axis perpendicular to the interface plane and E_i is the electric field between the donor impurities and two-dimensional electron gas [4]. Typically, one has for $\hbar^2 K = (1–10) \times 10^{-7}$ meV cm [5–7]. Apart from the Rashba SOI, there is an additional contribution caused by the inhomogeneous (confinement) potential that forms a billiard [8, 9]. However, if the confinement potential is approximated by hard walls, this contribution to the SOI can be ignored [9].

We use the billiard size R as the characteristic scale to rewrite Eq. (1) in the dimensionless form

$$\tilde{H} = \begin{pmatrix} -\nabla^2 & \beta\left(-\frac{\partial}{\partial x} + i\frac{\partial}{\partial y}\right) \\ \beta\left(\frac{\partial}{\partial x} + i\frac{\partial}{\partial y}\right) & -\nabla^2 \end{pmatrix}, \qquad (2)$$

where $\beta = 2m^*KR$ and all dimensionless coordinates are normalized to R. Then the Schrödinger equation for the spinor components takes the form

$$\begin{aligned} -\nabla^2\phi + \beta L\chi &= \epsilon\phi, \\ -\nabla^2\chi + \beta L^+\phi &= \epsilon\chi, \end{aligned} \qquad (3)$$

where the operator $L = -\partial/\partial x + i(\partial/\partial y)$. Problem (3) was studied in great detail for the systems without SOI (see, e.g., Stöckmann's monograph [10] or review [2]). Historically, McDonnel and Kaufmann [11] were the first to discover numerically that the complex spatial structure of real Bunimovich billiard eigenfunctions is described by the Gaussian distribution. The density probability (square of eigenfunction) statistics obeys the Porter–Thomas distribution [12]. These statistics were repeatedly observed in microwave [10, 13] and acoustic resonant [14] cavities.

In this work, we examine what happens to the statistics of two-component eigenfunctions in the presence of SOI. The energy-level statistics of a rectangular billiard, which becomes nonintegrable in the presence of SOI, was considered by Berggren and Ouchterlony in [15]. In that work, the eigenfunction node statistics were also considered and it was shown that they coincide with the statistics of nodal points of open chaotic billiards. For the numerical solution, we will use the boundary integral method [16]. A chaotic billiard was modeled by a cardioid with the boundary determined by the following equation in the Cartesian coordinate system [17]:

$$(x^2 + y^2 - \lambda^2)^2 = x^2 + y^2 + 2\lambda x + \lambda^2. \qquad (4)$$

The Bunimovich stadium was also considered. Since all results obtained for the latter do not differ from the cardioid, we present here only the cardioid results. The

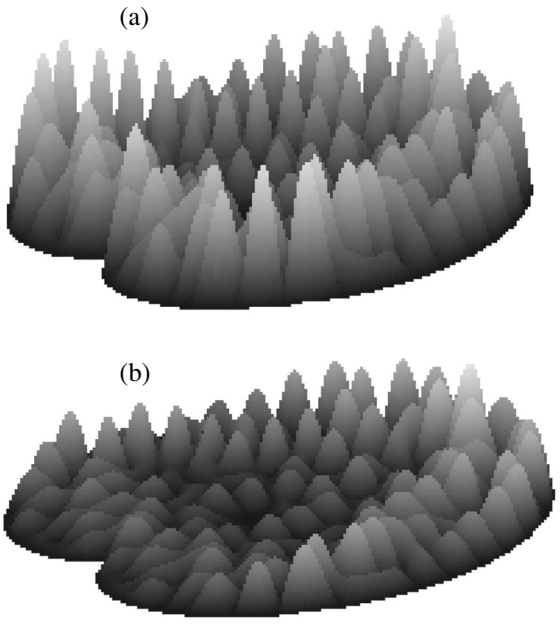

Fig. 1. Spatial structures of (a) the first $|\phi|$ and (b) the second $|\chi|$ components of the spinor eigenfunction of a cardioid with parameter $\lambda = 0.45$ for $\epsilon = 522.251$ and $\beta = 0.25$. The smallness parameter $\alpha = 0.005$.

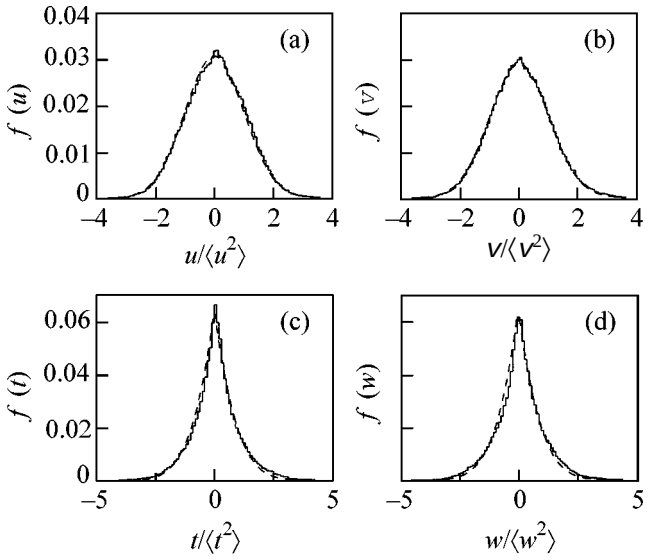

Fig. 2. Distributions of the real and imaginary parts of spinor components (7) for $\epsilon = 2509.7$ and $\beta = 0.25$. The smallness parameter $\alpha = 0.005$. The dashed curves in (a) and (b) correspond to Gaussian distribution (9). In panels (c) and (d), the dashed curves correspond to distribution (10) for $x_0 = -0.3$ and $y_0 = 0.4$.

spinor components $|\phi|$ and $|\chi|$ for the energy eigenvalue $\epsilon = 522.251$ and $\beta = 0.25$ are shown in Fig. 1. Hereafter, the cardioid parameter λ is taken to be 0.45. The number of boundary elements was chosen to be 1000. Note that, due to the Kramers theorem, all states of closed billiards with SOI are doubly degenerate. For this reason, the second degenerate state behaves exactly as shown in Fig. 1, although $|\phi|$ and $|\chi|$ should be reversed.

Although both components show chaotic behavior, there is a fundamental difference in their spatial behavior. Namely, one can see from Fig. 1 that the $|\chi|$ component is spatially nonuniform. This fact can be understood if one considers the perturbative solutions to the Schrödinger equation (3). For a free two-dimensional electron gas, the smallness parameter for SOI is given by [8]

$$\alpha = \beta k/\epsilon = \beta/\sqrt{\epsilon}, \tag{5}$$

where k is the wave number. We will use the same parameter for a billiard. For small α, the solution to Eqs. (3) can be approximated by

$$\begin{aligned} \phi &= \psi_b + O(\alpha^2), \\ \chi &= \beta\left[\frac{1}{2}(x+iy)\psi_b + C\psi_b\right] \\ &= \frac{\beta}{2}[(x-x_0)+i(y-y_0)]\psi_b, \end{aligned} \tag{6}$$

where ψ_b is the billiard eigenfunction in the absence of SOI: $-\nabla^2\psi_b = \epsilon_b\psi_b$. At first glance, the constant C can be found from the normalization condition $\int d^2\mathbf{x}(|\phi|^2 + |\chi|^2) = 1$. However, since the accuracy of the components is proportional to the SOI constant, the normalization condition includes only ψ_b that is already normalized. Because of this, the constant C (more precisely, the constants x_0 and y_0) was determined by fitting the statistics together (see below).

Solution (6) demonstrates that the second component $\chi(x, y)$ linearly increases in the billiard region, as it is clearly seen from the numerical solution shown in Fig. 1. It also follows from Eq. (6) that, if ψ_b is a random Gaussian field (RGF), the first component ϕ is also an RGF, whereas the second component χ is not. Since, in the presence of SOI, each component of the spinor eigenfunction is a complex quantity, we can represent the solution in the form

$$\begin{pmatrix} \phi(\mathbf{r}) \\ \chi(\mathbf{r}) \end{pmatrix} = \begin{pmatrix} u(\mathbf{r}) + iv(\mathbf{r}) \\ t(\mathbf{r}) + iw(\mathbf{r}) \end{pmatrix}. \tag{7}$$

The distributions shown in Fig. 2 for all four functions demonstrate that u and v are actually the RGF, whereas the t and w statistics differ appreciably from the Gaussian distributions.

To analytically derive the distributions for the second component χ, we write, according to Eq. (6), its real part as $t(x, y) = (\beta/2)(x - x_0)\psi_b$ and the imaginary

part as $w(x, y) = (\beta/2)(y - y_0)\psi_b$. The distribution function for t is written as

$$f(t) = \langle \delta(t - t(x, y)) \rangle = \frac{1}{2\pi}\int_{-\infty}^{\infty} d\mu \langle e^{i\mu(t - t(x, y))} \rangle = \frac{1}{2\pi}\int_{-\infty}^{\infty} d\mu \frac{1}{A}\int dx dy e^{i\mu(t - t(x, y))}, \quad (8)$$

where A is the billiard area. Assume that the eigenfunction ψ_b of a chaotic billiard is a real RGF $u(x)$. Then, by integrating Eq. (8) with the Gaussian distribution

$$f(u) = \sqrt{\frac{2\pi}{\langle u^2 \rangle}} \exp\left(-\frac{u^2}{2\langle u^2 \rangle}\right), \quad (9)$$

one obtains from Eq. (6)

$$f(t) = \frac{1}{A}\int dx dy \exp\left\{-\frac{2t^2}{\beta^2 (x - x_0)^2 \langle u^2 \rangle}\right\}. \quad (10)$$

A similar expression can be obtained for the distribution $f(w)$ of the imaginary part. Hence, the distributions for the second component χ are not universal if the Rashba SOI constant β is small, because they depend on the particular shape of a chaotic billiard. In Fig. 2, distribution (10) obtained by the numerical integration with $\beta = 0.25$ is shown by the dashed line. The constants x_0 and y_0 were found by fitting analytic distributions (10) to their numerical values. The results presented in the caption to Fig. 2 coincide with the results obtained for the constant C through the direct numerical solution of Eq. (2).

The numerically calculated matrix

$$K = \begin{pmatrix} \langle u^2 \rangle & \langle uv \rangle & \langle ut \rangle & \langle uw \rangle \\ \langle vu \rangle & \langle v^2 \rangle & \langle vt \rangle & \langle vw \rangle \\ \langle tu \rangle & \langle tv \rangle & \langle t^2 \rangle & \langle tw \rangle \\ \langle wu \rangle & \langle wv \rangle & \langle wt \rangle & \langle w^2 \rangle \end{pmatrix} = \begin{pmatrix} 0.292 & 0.038 & -0.024 & -0.015 \\ 0.038 & 0.198 & -0.015 & 0.011 \\ -0.024 & -0.015 & 0.005 & 0 \\ -0.015 & 0.011 & 0 & 0.004 \end{pmatrix}, \quad (11)$$

where $\langle F \rangle = \frac{1}{N}\sum_j F(j)$ and N is the number of points inside the billiard (200 000 in these computations) indicates that the second component is strongly correlated with the first one. In the numerical computations, we assumed that the eigenstate is normalized; i.e., $\sum_j (|\phi(j)|^2 + |\chi(j)|^2) = 1$.

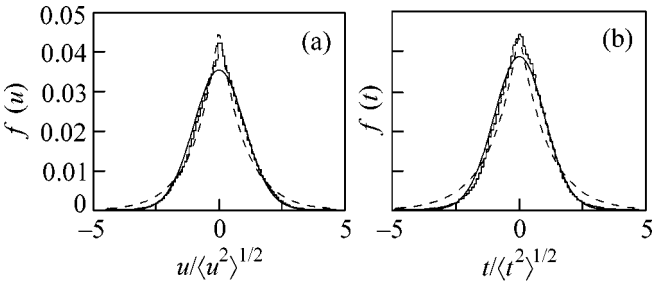

Fig. 3. Distributions of the real parts of the cardioid eigenstates for $\epsilon = 2501.6$ and $\beta = 2$. The SOI smallness parameter is $\alpha = 0.04$. The solid curves correspond to Gaussian distribution (9). The dashed curves correspond to distribution (10) for $x_0 = -0.050$.

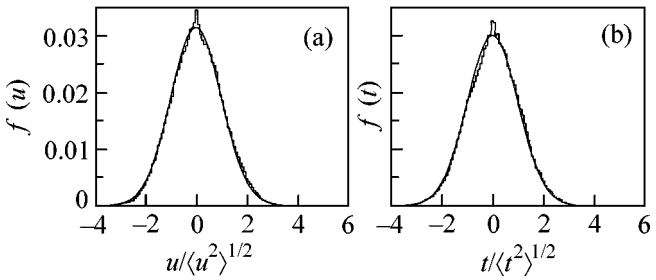

Fig. 4. Distributions of the real part of the cardioid eigenstates for $\epsilon = 2497.4$, $\beta = 10$, and $\alpha = 0.2$. The solid curves correspond to Gaussian distribution (9).

The distributions of real components u and t of spinor eigenstate (7) are shown in Fig. 3 for a moderate value $\beta = 2$ of the SOI constant. These distributions indicate that, with an increase in small parameter α, the statistics remains Gaussian for large wave-function amplitudes and is added by nonuniversal statistics (10) at small amplitudes. The statistics of the imaginary parts v and w are exactly the same as for the real eigenstate parts. For this reason, they are not shown in Fig. 3 (or Fig. 4).

In the opposite case $\alpha \gg 1$, one can ignore the kinetic energy operators in Eq. (3). Then, surprising as it may seem, Schrödiner equation (3) again reduces to the Laplace equation for both components ϕ and χ

$$L^+ L \begin{pmatrix} \phi \\ \chi \end{pmatrix} = -\nabla^2 \begin{pmatrix} \phi \\ \chi \end{pmatrix} = \beta^2 |\epsilon|^2 \begin{pmatrix} \phi \\ \chi \end{pmatrix} \quad (12)$$

with the sole difference that the eigenvalues are now equal to $\beta^2\epsilon^2$. Hence, both components are equivalent in that they are RGFs with identical variances. The numerical solutions for $\beta = 100$ fully confirm this conclusion. However, at $\beta \geq 10$, all four functions in eigenspinor (7) are, practically, RGFs, as it is seen from Fig. 4.

Correlation matrix (11) was calculated for $\epsilon = 2499.2$, $\beta = 10$, and $\alpha = 0.2$ to give

$$K = \begin{pmatrix} 0.248 & -0.042 & 0.047 & 0 \\ -0.042 & 0.243 & 0 & 0.047 \\ 0.047 & 0 & 0.253 & 0.021 \\ 0 & 0.047 & 0.021 & 0.255 \end{pmatrix}. \quad (13)$$

This matrix shows that, at $\beta \geq 10$, all amplitudes become almost mutually independent RGFs with the same distributions.

We now estimate the small parameter α for the quantum dots based on the semiconductor GaSb/InAs/GaSb heterostructure, for which the SOI constant is the greatest among the known systems: $\hbar^2 K = 9 \times 10^{-7}$ meV cm and $m^* = 0.055m$ [5]. Substituting these data into the SOI constant $\beta = 2m^*KR = \hbar^2 K/E_0 R$ and $E_0 = \hbar^2/2m^*R^2$, one finds that only the quantum dots with sizes $R \sim 10$ μm have $\beta \sim 10$, for which, as shown in Fig. 4, all eigenspinor components are described by the RGF. The electron Fermi energy in the dot should not exceed 1 meV. Note that $R \sim 10$ μm is the limiting attainable size for which the electron motion can be assumed to be ballistic. For the quantum dots of micron size or smaller, the eigenfunction statistics in spin–orbit problem (1) are described by nonuniversal distribution (10).

This work was supported by the Russian Foundation for Basic Research, project nos. 01-02-16077 and 03-02-17039. One author is grateful to Prof. Karl-Fredrik Berggren (Linköping University, Sweden) for discussions.

REFERENCES

1. J. H. Davies, *The Physics of Low-Dimensional Semiconductors* (Cambridge Univ. Press, Cambridge, 1998).
2. Y. Alhassid, Rev. Mod. Phys. **72**, 895 (2000).
3. E. I. Rashba, Fiz. Tverd. Tela (Leningrad) **2**, 1224 (1960) [Sov. Phys. Solid State **2**, 1109 (1960)].
4. E. A. de Andrada e Silva, G. C. La Rocca, and F. Bassani, Phys. Rev. B **55**, 16293 (1997).
5. J. Luo, H. Munekata, F. F. Fang, and P. J. Stiles, Phys. Rev. B **41**, 7685 (1990).
6. J. Nitta, T. Akasaki, H. Takaynagi, and T. Enoki, Phys. Rev. Lett. **78**, 1335 (1997).
7. J. P. Heida, B. J. van Wees, J. J. Kuipers, *et al.*, Phys. Rev. B **57**, 11911 (1988).
8. A. V. Moroz and C. H. W. Barnes, Phys. Rev. B **60**, 14272 (1999).
9. E. N. Bulgakov and A. F. Sadreev, Phys. Rev. B **66**, 075331 (2002).
10. H.-J. Stöckmann, *Quantum Chaos: An Introduction* (Cambridge Univ. Press, Cambridge, 1999).
11. S. W. McDonald and A. N. Kaufmann, Phys. Rev. Lett. **42**, 1189 (1979); Phys. Rev. A **37**, 3067 (1988).
12. N. Rosenzweig and R. Thomas, Phys. Rev. **120**, 1698 (1960).
13. A. Kudrolli, V. Kidambi, and S. Sridhar, Phys. Rev. Lett. **75**, 822 (1995).
14. K. Schaadt, MS Thesis (The Niels Bohr Inst., Univ. of Copenhagen, 1997).
15. K.-F. Berggren and T. Ouchterlony, Found. Phys. **31**, 233 (2001).
16. R. J. Riddel, Jr., J. Comput. Phys. **31**, 21 (1979); J. Comput. Phys. **31**, 42 (1979).
17. M. Robnik, J. Phys. A: Math. Gen. **16**, 3971 (1983).

Translated by V. Sakun